ORIGINAL ARTICLE

HPV8 Field Cancerization in a Transgenic Mouse Model Is due to Lrig1+ Keratinocyte Stem Cell Expansion

Simone Lanfredini[1,5], Carlotta Olivero[2,5], Cinzia Borgogna[2], Federica Calati[2], Kathryn Powell[1], Kelli-Jo Davies[1], Marco De Andrea[2,3], Sarah Harries[1], Hiu Kwan Carolyn Tang[1], Herbert Pfister[4], Marisa Gariglio[2,6] and Girish K. Patel[1,6]

β-Human papillomaviruses (HPVs) cause near ubiquitous latent skin infection within long-lived hair follicle (HF) keratinocyte stem cells. In patients with epidermodysplasia verruciformis, β-HPV viral replication is associated with skin keratosis and cutaneous squamous cell carcinoma. To determine the role of HF keratinocyte stem cells in β-HPV-induced skin carcinogenesis, we utilized a transgenic mouse model in which the keratin 14 promoter drives expression of the entire HPV8 early region (HPV8tg). HPV8tg mice developed thicker skin in comparison with wild-type littermates consistent with a hyperproliferative epidermis. HF keratinocyte proliferation was evident within the Lrig1+ keratinocyte stem cell population (69 vs. 55%, $P < 0.01$, $n = 7$), and not in the CD34+, LGR5+, and LGR6+ keratinocyte stem cell populations. This was associated with a 2.8-fold expansion in Lrig1+ keratinocytes and 3.8-fold increased colony-forming efficiency. Consistent with this, we observed nuclear p63 expression throughout this population and the HF infundibulum and adjoining interfollicular epidermis, associated with a switch from p63 transcriptional activation isoforms to ΔNp63 isoforms in HPV8tg skin. Epidermodysplasia verruciformis keratosis and in some cases actinic keratoses demonstrated similar histology associated with β-HPV reactivation and nuclear p63 expression within the HF infundibulum and perifollicular epidermis. These findings would suggest that β-HPV field cancerization arises from the HF junctional zone and predispose to squamous cell carcinoma.

Journal of Investigative Dermatology (2017) **137,** 2208–2216; doi:10.1016/j.jid.2017.04.039

INTRODUCTION

More than 200 human papillomavirus (HPV) types have been DNA sequenced and thus classified into five genera (*Alpha-*, *Beta-*, *Gamma-*, *Mu-*, and *Nu-papillomavirus*) (Bernard et al., 2010; http://pave.niaid.nih.gov/#home). High-risk α-HPV types have been established to be causative for cancer, notably in the anogenital tract (Bosch et al., 2013). In contrast, β-HPV types are evolutionarily distinct as they do not integrate into the host genome and cause ubiquitous latent skin infection (Quint et al., 2015). The likely reservoir for β-HPV latent infection is postulated to reside within long-lived hair follicle keratinocyte stem cells (HF-KSC), because plucked hair consistently demonstrates β-HPV DNA and KSC characteristics are enhanced by HPV 5 and 8 early region genes (Bouwes Bavinck et al., 2008; Boxman et al., 1997; Hufbauer et al., 2013). However, the precise HF-KSC populations involved in β-HPV latent infection remain to be defined (Kranjec and Doorbar, 2016). Markers of β-HPV infection are uniformly observed in epidermodysplasia verruciformis (EV) keratosis and cutaneous squamous cell carcinoma (SCC), which represents the prototypic model of β-HPV-induced skin carcinogenesis (Borgogna et al., 2012, 2014a). EV is a rare genodermatosis that has been included in the list of primary immunodeficiencies characterized by defects in innate immunity (Notarangelo et al., 2004). Inactivating biallelic mutations of either EVER1/TMC6 or EVER2/TMC8 have been described in several families suffering from EV and account for about half of described EV cases (Ramoz et al., 2002). Atypical cases of EV have also been reported and they usually display T-cell defects (Azzimonti et al., 2005; Borgogna et al., 2014a; Landini et al., 2014). It has been postulated that β-HPV reactivation is also associated with skin carcinogenesis in organ transplant recipients (Borgogna et al., 2014b; Howley et al., 2015; Quint et al., 2015). To determine the role of HF-KSC in β-HPV-induced skin carcinogenesis, we utilized a transgenic mouse model in which the entire HPV8 early region genes are expressed under a keratin 14 promoter (HPV8tg) (De Andrea et al., 2010; Schaper et al., 2005). HPV8tg mice develop

[1]*European Cancer Stem Cell Research Institute, School of Biosciences, Cardiff University, Cardiff, UK;* [2]*Virology Unit, Department of Translational Medicine, Novara Medical School, Novara, Italy;* [3]*Viral Pathogenesis Unit, Department of Public Health and Pediatric Sciences, Turin Medical School, Turin, Italy; and* [4]*Institute of Virology, University of Cologne, Cologne, Germany*

[5]*These authors contributed equally to this work.*

[6]*These senior authors contributed equally to this work.*

Correspondence: Girish K. Patel, European Cancer Stem Cell Research Institute, School of Biosciences, Cardiff University, Maindy Road, Cardiff CF24 4HQ, UK. E-mail: patelgk@cardiff.ac.uk

Abbreviations: AK, actinic keratosis; EV, epidermodysplasia verruciformis; HF, hair follicle; HPV, human papillomavirus; IFE, interfollicular epidermis; KSC, keratinocyte stem cell; SCC, cutaneous squamous cell carcinoma; TA, transcriptional activation; WT, wild type

Received 1 December 2016; revised 25 April 2017; accepted 28 April 2017; accepted manuscript published online 5 June 2017; corrected proof published online 8 July 2017

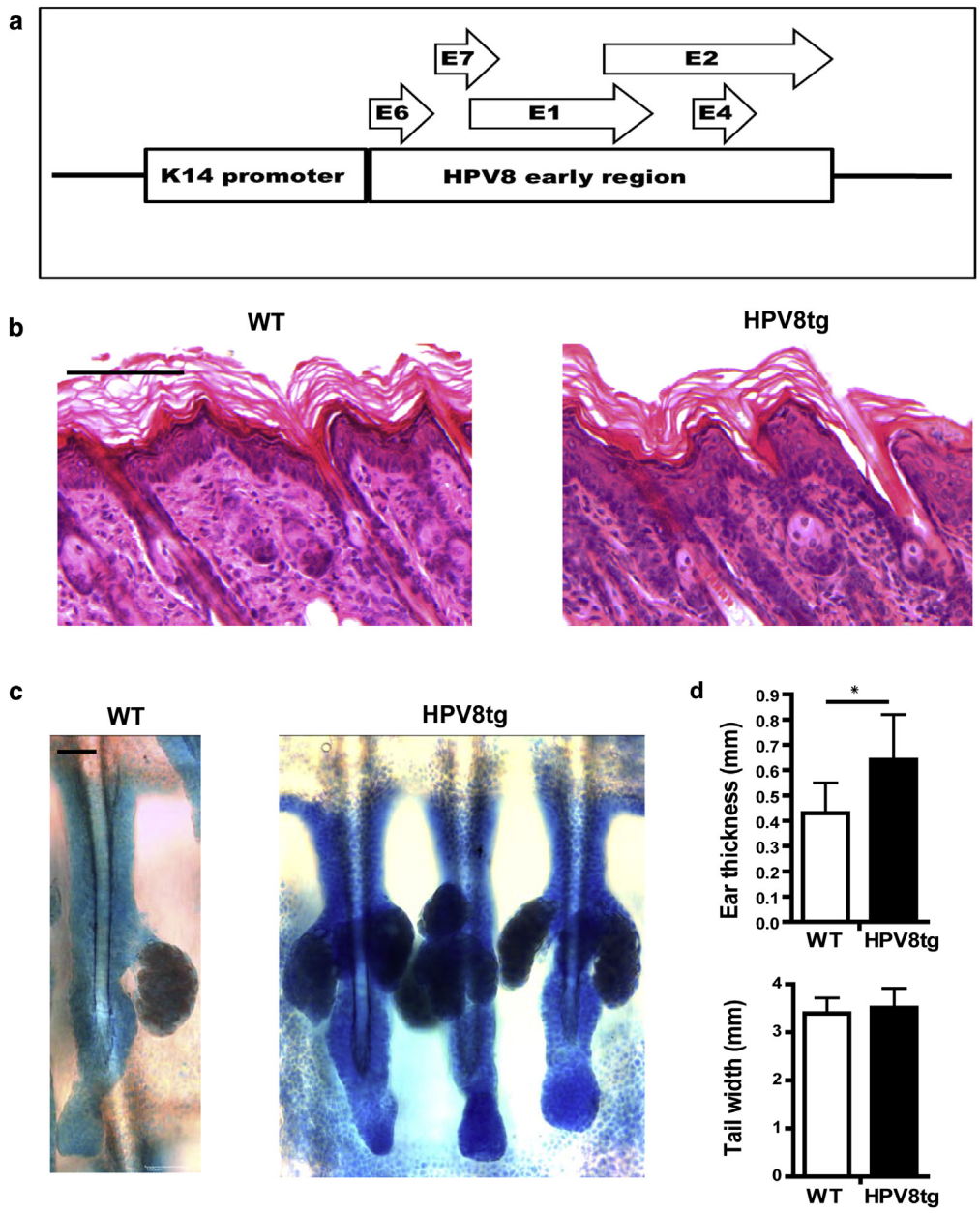

Figure 1. Phenotypic and histological characterization of HPV8tg mice. (**a**) Schematic representation of the HPV8 transgenes, showing the human cytokeratin-14 gene promoter upstream of the open reading frames of the HPV8 early region genes. (**b**) Hematoxylin and eosin staining of paraffin-embedded skin sections from WT (left panel) and HPV8tg (right panel) mouse skin. (**c**) Toluidine blue staining of mouse whole mount skin including the hair follicle and overlying epidermis from WT (left panel) and HPV8tg (right panel) from the tail. (**d**) Ear thickness (upper graph) and tail width (bottom graph) measured using calipers on age-matched WT and HPV8tg littermates (n = 8), with mean ± SD (*$P < 0.05$; unpaired *t* test). All the images were processed using ImageJ software (National Institutes of Health, Bethesda, MD). All scale bars = 100 μm. HPV, human papillomavirus; SD, standard deviation; WT, wild type.

multiple persistent papillomas within 8 weeks, of which 6% go on to develop spontaneous SCC with metastatic potential.

In this study, we provide a model of β-HPV-induced skin carcinogenesis that is based on the aberrant expansion of Lrig1+ KSC in the upper hair follicle that spill out into the surrounding epidermis. Similarly expansion of the junctional zone HF KSC population was identified by p63 labeling in human EV keratosis and actinic keratosis (AK).

RESULTS

The HPV8tg mice skin displays HF proliferative epidermal hyperplasia

After birth, HPV8tg mice develop thicker skin in comparison with wild-type (WT) littermates (Figure 1). Adult HPV8tg skin thickness of the ear was 0.6 ± 0.1 versus 0.4 ± 0.1 mm ($P < 0.05$, n = 9); there was no difference in weight and tail width. More keratinocyte layers were evident in the HF infundibulum and adjoining interfollicular epidermis (IFE) in HPV8tg, 4.2 ± 0.47 versus 2.0 ± 0.0 and 3.8 ± 0.49 versus 1.5 ± 0.43, respectively ($P < 0.01$, n = 5), but stratum corneum thickness measured on histological sections was not different. Consistent with a hyperproliferative epidermis, keratinocyte proliferation assessed by Ki67 positive cells per basal keratinocyte was markedly increased within the HF (41± 10.9 vs. 23 ± 11.8, n = 7, $P = 0.01$) and to a lesser extent the IFE (0.46 ± 0.18 vs. 0.31 ± 0.11, n = 15, $P = 0.01$). The expression of HPV8 early region genes in this transgenic mouse model has been previously described (De Andrea et al., 2010; Schaper et al., 2005). Whereas this HPV8tg mouse model yields spontaneous SCC formation, other similar β-HPV transgenic models driven by K14 promoter do

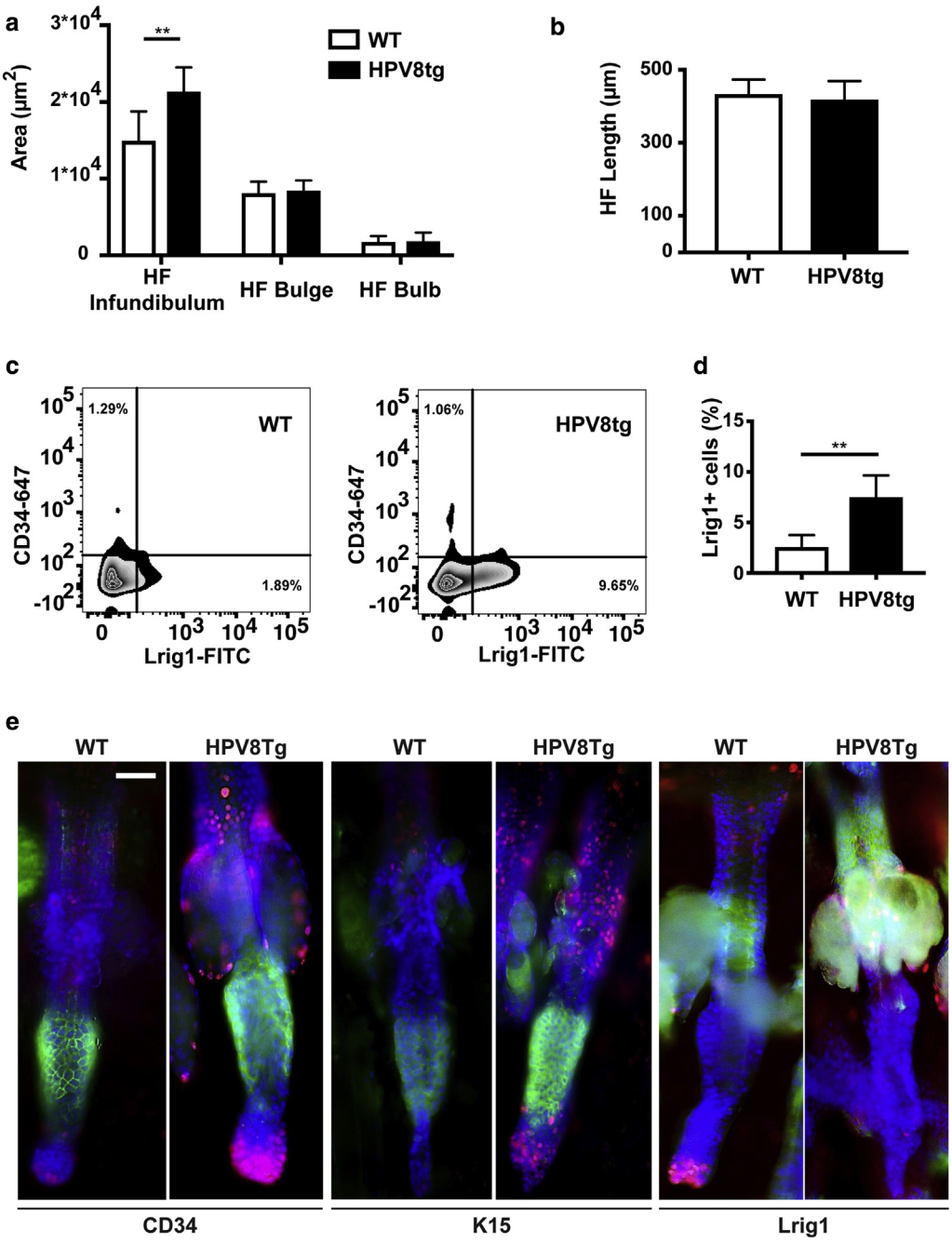

Figure 2. HPV8 transgenes induce hair follicle changes in HPV8tg mice. (**a, b**) Adult mice whole mount skin was photographed and analyzed for the area of HF regions and length, WT and HPV8tg were compared, with mean ± SD, using an unpaired *t* test (n = 20, $^{**}P < 0.01$). (**c**) FACS analysis WT and HPV8tg mice skin keratinocyte isolates (n = 6), labeled with Lrig1-FITC and CD34-647 antibodies, with DAPI to select live cells. (**d**) The number of Lrig1 positive cells determined by FACS (n = 6). ($^{**}P < 0.01$; unpaired *t* test), with mean ± SD. (**e**) Whole mount immunofluorescence of adult WT and HPV8tg tail skin for Ki67 (red) and HF-KSC markers (green). All the images were processed using ImageJ software (National Institutes of Health, Bethesda, MD). All scale bars = 100 μm. HF, hair follicle; HPV, human papillomavirus; KSC, keratinocyte stem cell; SD, standard deviation; WT, wild type.

not develop SCC spontaneously (Viarisio et al., 2011). Consistent with this, levels of E6 and E7 expression in HPV8tg mouse skin were similar to that observed in HeLa cells with natural HPV18 infection (Supplementary Figure S1 online). Together these findings suggested that HPV8 early region genes induce a proliferative epidermal hyperplasia, notably in the HF. HPV8-induced keratinocyte proliferation was greatest in the HF and immediately adjoining IFE, as determined by Ki67 expression, even though keratin 14 promoter-driven HPV8 early region genes were uniformly expressed.

The Lrig1 KSC population is expanded in HPV8tg mice

Within the HF, the mean area of the infundibulum was markedly increased in HPV8tg compared with WT mice (Figure 2a), whereas there was no difference in HF length (Figure 2b).

To determine which hair follicle keratinocyte population becomes expanded in HPV8tg mice compared with WT littermates, we labeled skin sections in whole mount analysis with a set of stem cell markers. Consistent with the observed HF infundibulum expansion, keratinocyte proliferation was evident within the Lrig1+ KSC population (69% vs. 55%, $P < 0.01$, n = 7), and not in the CD34+ (1% vs. 1%), LGR5+ (1% vs. 3%) and LGR6+ (29% vs. 40%) KSC populations (n = 7, Figures 2c–e, 3a, and 3b). Flow cytometric analysis of dissociated skin confirmed a 2.8-fold increase in Lrig1+ keratinocytes in the HPV8tg mice, 7.4% ± 2.2% versus 2.7% ± 0.8%, n = 6, $P < 0.05$, but no difference in CD34+ KSC

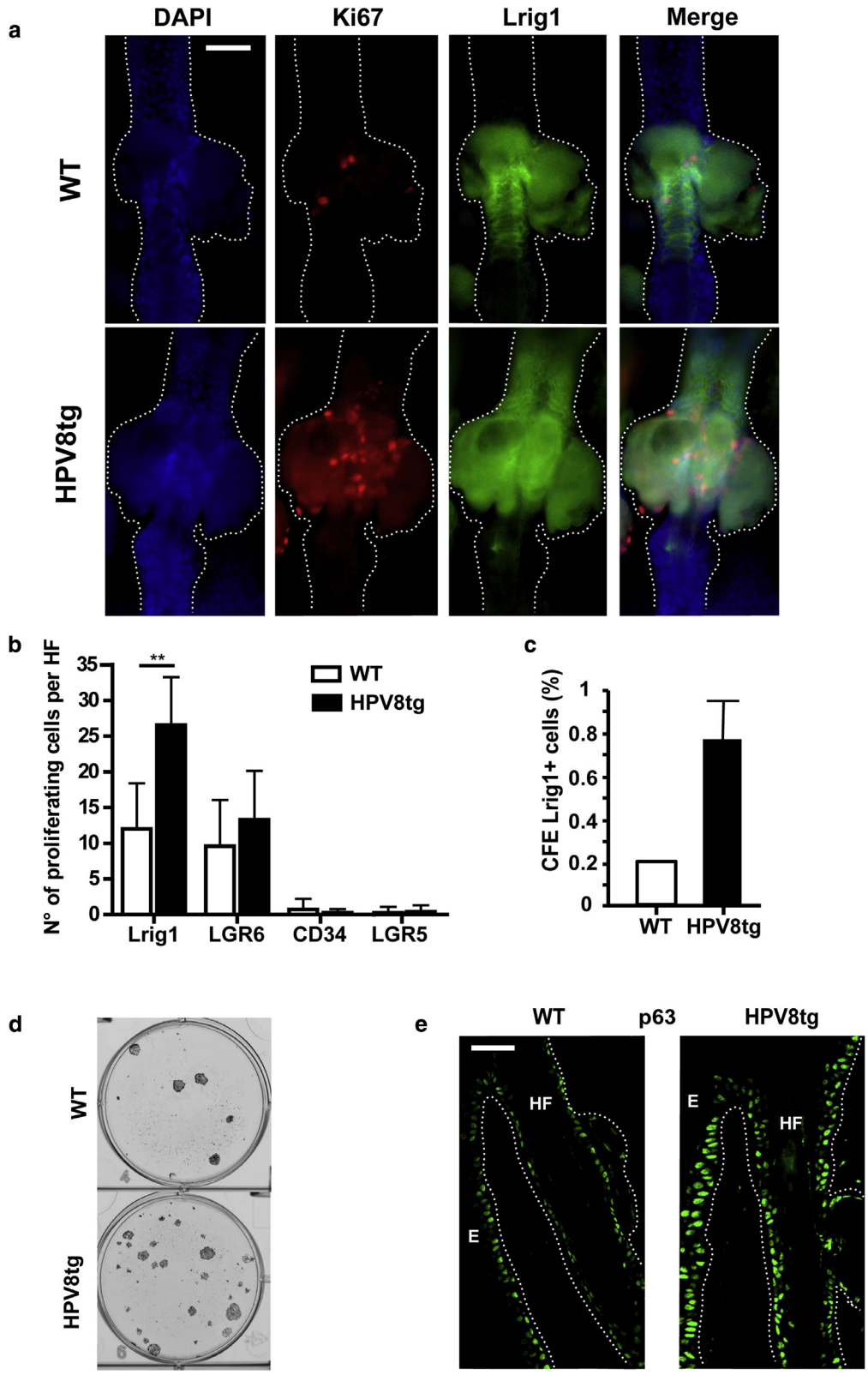

Figure 3. Lrig1 keratinocyte stem cell proliferation in HPV8tg. (**a**) Whole mount adult WT and HPV8tg (n = 6) skin sections labeled with Ki67 (red), Lrig1 (green) antibodies, and DAPI (blue). (**b**) Number of proliferating cells within KSC populations (Lrig1, LGR6, CD34, and LGR5) was enumerated, with mean ± SD, in WT and HPV8tg tissue sections (n = 7); $^{**}P < 0.01$. (**c**) Keratinocyte colony-forming assays from flow sorted Lrig1 cells from WT and HPV8tg (n = 6) skin dissociates, with mean ± SD. (**d**) A representative image. (**e**) p63 labeled frozen sections from adult WT and HPV8tg mice (n = 3); the broken line indicates the basal layer. Immuno-labeled tissue sections were visualized and photographed by a fluorescent microscope with ×20 magnification and then processed using ImageJ software (National Institutes of Health, Bethesda, MD). All scale bars = 100 μm. HF, hair follicle; HPV, human papillomavirus; KSC, keratinocyte stem cell; SD, standard deviation; WT, wild type.

numbers (0.81% ± 0.24% vs. 0.73% ± 0.37%) (Figure 2c). Flow sorted Lrig1+ and CD34+ keratinocyte subpopulations had similar levels of K14 promoter-driven early region gene mRNA expression (Figure 4a), despite the observed difference in proliferation. To exclude any difference in the *EVER 1* and *2* gene expression levels in HPV8tg mice versus control, real-time quantitative reverse transcription analysis was performed with the RNA extracted from Lrig1+ sorted cells and found comparable levels as shown in Figure 4b. Flow sorted Lrig1+ keratinocytes from HPV8tg mice also demonstrated a

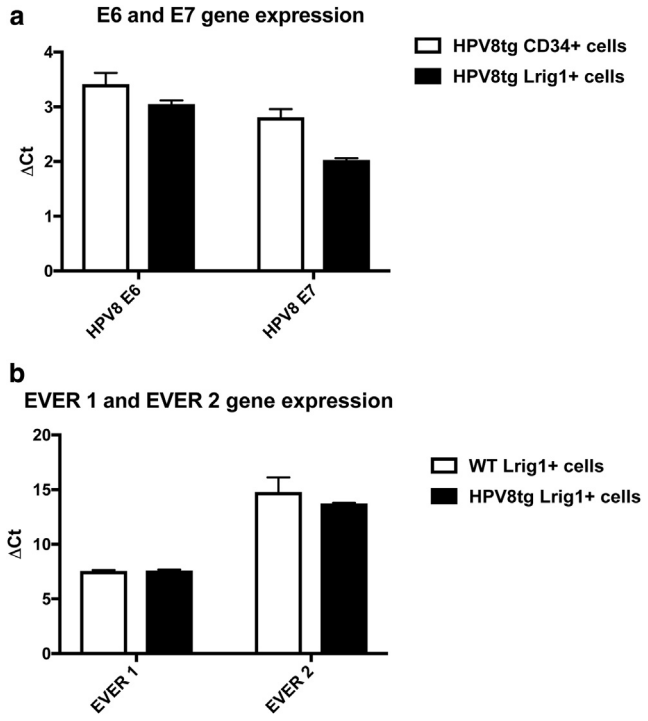

Figure 4. HPV8 transgenes are uniformly expressed in the epidermis of HPV8tg mice. (**a**) qRT-PCR of early region genes of WT and HPV8tg mouse skin isolated KSC populations, with mean ± SD. (**b**) qRT-PCR of murine homologs of *EVER1 (TMC6)* and *EVER2 (TMC8)* genes of WT and HPV8tg mouse skin isolated Lrig1+ KSC populations, with mean ± SD. HPV, human papillomavirus; KSC, keratinocyte stem cell; qRT-PCR, real-time quantitative reverse transcription analysis; SD, standard deviation; WT, wild type.

3.8-fold increased colony-forming efficiency (Figure 3c, 3d); hence Lrig1+ cells retain KSC function. There was no significant difference in colony-forming efficiency from flow sorted Lrig1 negative keratinocytes from HPV8tg versus WT mice (Supplementary Figure S2 online). In keeping with Lrig1+ expansion and proliferation, we observed nuclear p63 expression throughout this population and the emanating keratinocytes of HF infundibulum and adjoining IFE (Figure 3e). Reverse transcription-PCR and western blotting analysis confirmed the switch from p63 transcriptional activation (TA) isoforms to ΔNp63 isoforms in HPV8tg skin (Figure 5a–c), consistent with earlier reports indicating that HPV8 early proteins induce p63 expression (Meyers et al., 2013). Thus Lrig1+ KSC proliferation through induction of ΔNp63 in HPV8tg skin resulted in KSC expansion into the overlying infundibulum and adjoining IFE.

β-HPV associated expansion of the HF junctional zone KSC population in human skin field cancerization

The dilated HF infundibulum with increased keratinocyte layers and the crowded perifollicular epidermis with hyperkeratosis were consistently observed in the HPV8tg mice, and resembled Freudenthal's funnel, the pathognomonic histological finding in AK (n = 28 mice, Supplementary Figure S3 online). EV keratosis uniformly demonstrated similar histology associated with β-HPV reactivation and nuclear p63 expression within the HF infundibulum and perifollicular epidermis (Figure 5d, 6 patients with 44 lesions, Supplementary Table S1 online). Likewise, in some cases of AK from patients without EV, we were able to detect nuclear p63 expression within the infundibulum and perifollicular epidermis in areas where β-HPV reactivation was well evident, as detected by expression of the viral marker E4 (Figure 5d, n = 2 of 25). Hence, our findings suggest that similar to HPV8tg mice, patients with EV and some patients with AK demonstrate expansion of a junctional zone HF KSC population identified by p63 labeling. These findings would suggest that β-HPV field cancerization arises from the HF infundibulum and predispose to SCC. Indeed, we observed p63 positive cells in HPV8tg and human SCC (Figure 5e, n = 5); the latter were from immunocompetent patients from sun-exposed sites.

DISCUSSION

The concept of "field cancerization" as introduced by Slaughter et al. (1953) was initially used to describe an area of upper aerodigestive tract in situ SCC, within which develop multiple invasive SCC foci. In the skin, similar preneoplastic field cancerization is observed and is characterized by the presence of multiple AKs (Stockfleth et al., 2011). Although UV light-induced DNA damage is the prime cause of AK, other factors, including β-HPV infection, can also contribute to the development of this skin disorder, especially in immunocompromised patients (Banerjee et al., 2008; Taguchi et al., 1994; Weissenborn et al., 2005). Patients with EV and related primary T-cell immunodeficiency syndrome are predisposed to develop skin field cancerization with similar keratoses that are associated with reactivation of latent β-HPV infection (Azzimonti et al., 2005; Landini et al., 2014). In all cases of skin field cancerization, UV light is the key driver for transformation to SCC, as tumors typically arise on sun-exposed sites and contain p53 UV signature mutations (Jonason et al., 1996). Intriguingly, we have previously observed β-HPV reactivation at the clinically unaffected skin and in situ carcinoma at the periphery of SCC lesions from EV and organ transplant recipient, as well as within EV SCC (Borgogna et al., 2014b). In some cases, 2 of 25 cases studied of non-EV AK, β-HPV reactivation was observed. The HPV8tg mouse model with constitutive epithelial HPV8 expression develops keratosis like skin changes, with 6% of lesions progressing to spontaneous SCC (Schaper et al., 2005). The rate of conversion to SCC is greater in HPV8tg than in patients with EV and may reflect the higher expression of early region genes. As in human EV, UV radiation rapidly leads to SCC formation in HPV8tg and other HPV mouse models (Marcuzzi et al., 2009; Viarisio et al., 2011).

KSC reside within each compartment of the skin: the IFE, HF, sebaceous, and sweat glands. Different mouse KSC pools are distributed along the HF, defined by the expression of cell surface proteins that facilitate isolation and thus characterization. To date KSC have been identified within four HF regions: upper (Lrig1) and lower (LGR6) junctional zone, the bulge (CD34 and K15) and bulb (LGR5) (Kretzschmar and Watt, 2014; Solanas and Benitah, 2013) (Figure 6). In this study, we have identified the HF Lrig1+ KSC population as the putative target in HPV8tg mice skin carcinogenesis. Lrig1 expression defines a distinct multipotent stem cell population in mammalian epidermis, which resides in the HF junctional zone in mice (Jensen et al., 2009). Although Lrig1 expression

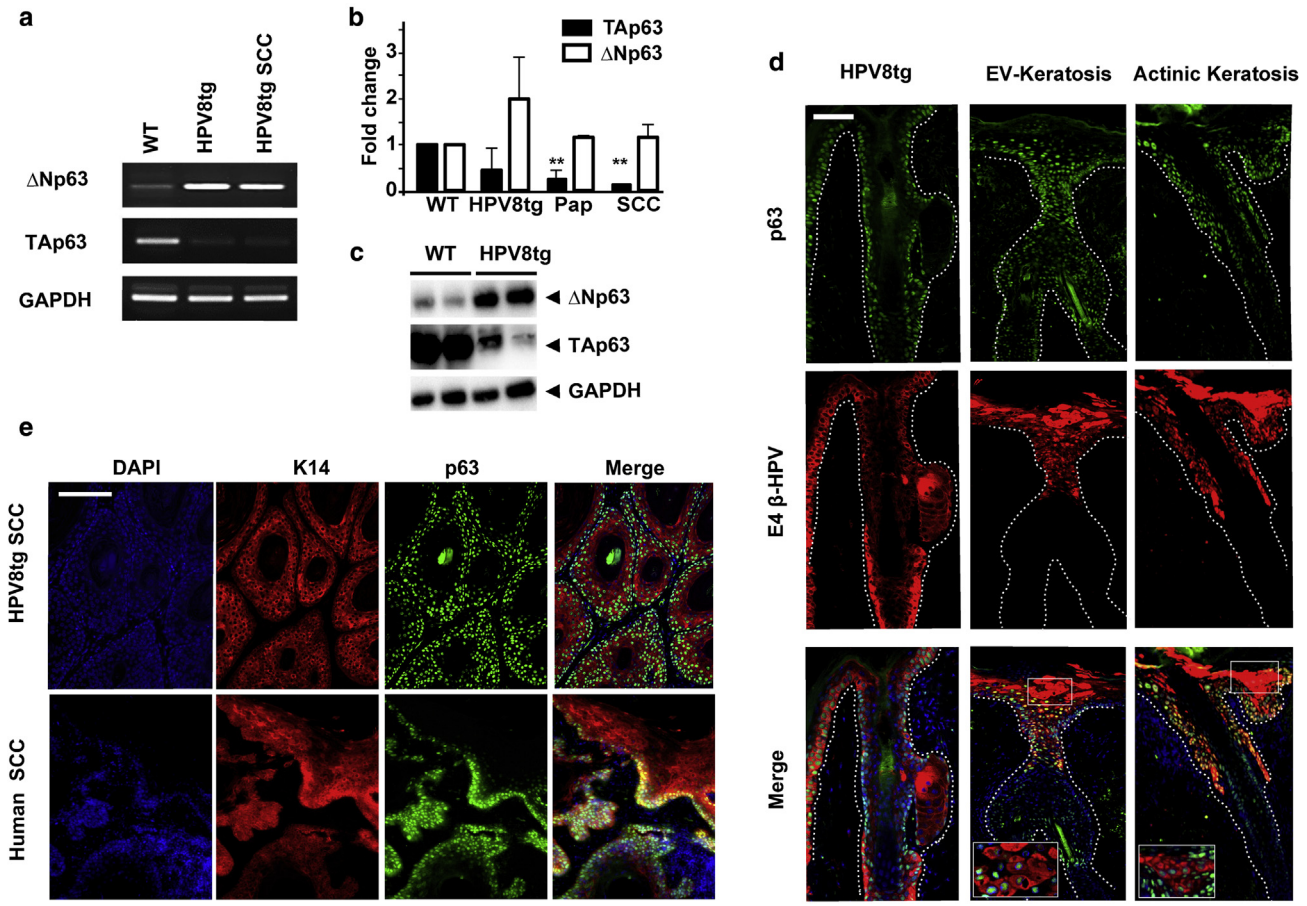

Figure 5. β-HPV-induced keratinocyte stem cell expansion results in keratosis that are predisposed to SCC. (**a, b**) Reverse transcription-PCR with mean ± SD (**$P < 0.01$) and (**c**) western blot gels of p63 isoforms from RNA and protein isolates respectively from WT, HPV8tg skin, papilloma (pap), and SCC (n = 6). (**d**) Images of tissue sections of HPV8tg mouse skin, human EV keratosis, and AK labeled with p63 (green), β-HPV E4 (red) specific antibodies, and DAPI (blue). (**e**) Images of tissue sections of HPV8tg mouse and human SCCs labeled with K14 (red), p63 (green) specific antibodies, and DAPI (blue). Immuno-labeled tissue sections were visualized and photographed by fluorescent microscope with ×20 magnification and then processed using ImageJ software (National Institutes of Health, Bethesda, MD). All scale bars = 100 μm. EV, epidermodysplasia verruciformis; GAPDH, glyceraldehyde-3-phosphate dehydrogenase; HPV, human papillomavirus; SCC, cutaneous squamous cell carcinoma; SD, standard deviation; WT, wild type.

defines an IFE KSC population in humans, it is not expressed in the reciprocal HF junctional zone (Supplementary Figure S4 online) and so prevented further characterization of the β-HPV target in humans (Jensen and Watt, 2006). Reporter mice studies have shown that junctional zone Lrig1+ cells give rise to keratinocytes in the infundibulum and adjoining IFE, akin to the expansion of this population in our HPV8tg mice, human EV keratosis, and AK.

p63 is a p53 protein family member expressed primarily in epithelia as six distinct isoforms, due to alternative transcription and C terminus splicing (Yang et al., 1998). Three p63 isoforms contain an N-terminal TA isoform sequence, whereas the other three do not (ΔN isoforms). All of the p63 isoforms, TA and ΔN, are transcriptionally active and the ΔN isoforms repress TA isoforms as dominant-negative molecules (Koster, 2010). Multiple lines of evidence support the role of p63 in KSC maintenance (Melino et al., 2015): (i) p63 null mice demonstrate a terminally differentiated epidermis with no proliferative basal layer containing stem cells (Yang et al., 1999); (ii) epidermal p63 knockdown induces differentiation, which is induced by TAp63 (Truong et al., 2006); (iii) ΔNp63 expression maintains the proliferative basal layer (Truong et al., 2006); and (iv) p63 nuclear accumulation is prominent in KSC and holoclones (Pellegrini et al., 2001). UV directly and via p53 mutation results in p63 downregulation and loss of transcriptional activity (Liefer et al., 2000). Recently it has been proposed that UV-induced concomitant activation of oncogenic Ras and transforming growth factor-β pathways can restore p63 activity in p53 mutant cells to promote tumor progression (Vasilaki et al., 2016). In keeping with this, UV-induced AK and cutaneous SCC frequently demonstrate nuclear p63 (Abbas et al., 2011).

The frequency of nuclear p63 positivity is greater in HPV associated SCC of the oral and anogenital regions, promoted by HPV E6 degradation of p53 (Melino, 2011).

β-HPV early region genes E2, E6, and E7 can induce KSC proliferation through inhibition of Notch signaling and subsequent induction of p63 (Hufbauer et al., 2013; Meyers et al., 2013; Pfefferle et al., 2008) providing a putative mechanism for this β-HPV-induced field cancerization. Hence, we propose that β-HPV early region genes initiate proliferation of Lrig1+ KSC causing their expansion into the overlying HF infundibulum and overlying epidermis. β-HPV-driven KSC proliferation results in EV keratosis and

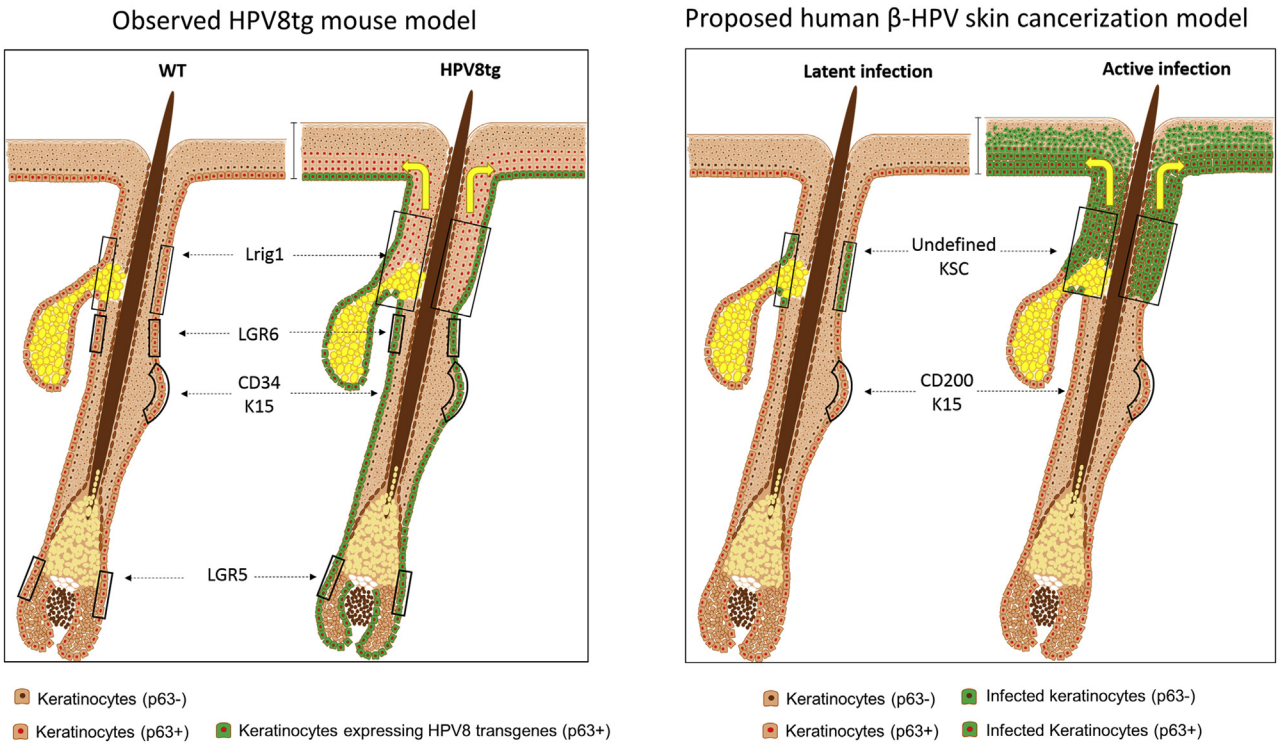

Figure 6. β-HPV field cancerization model. The mouse HF (left image) is composed of at least four different KSC populations. In the WT HF, the LGR5 is expressed in the hair bulb, CD34+ and K15+ KSC are located in the bulge, and the Lrig1 and LGR6 KSC are located in the upper and lower junctional zone, respectively. In HPV8tg, the Lrig1 KSC population expands beyond the junctional zone niche and no longer expresses Lrig1, but it maintains KSC function. Similarly, in human β-HPV reactivation (right image), the expanded population occupies the hair follicle infundibulum and adjoining interfollicular epidermis, as shown by the yellow arrow. These changes culminate in the histological phenotype known as Freudenthal's funnel, the pathognomonic finding in actinic keratosis and skin field cancerization. HF, hair follicle; HPV, human papillomavirus; KSC, keratinocyte stem cell; WT, wild type.

occasionally non-EV AK, which are predisposed to transformation into SCC whereupon the β-HPV episome and so gene expression is lost (Figure 6).

MATERIAL AND METHODS

Transgenic mouse model

HPV8tg and WT litter mates were housed and managed under conditions approved by the Italian Animal Care Committee. Age- and sex-matched mice ear thickness and tail width were measured using a Vernier caliper.

Whole mount skin preparation

Tail and back skin was cut into 0.5 cm^2 pieces and dissociated using 2.5 U/ml Dispase (Roche, Burgess Hill, UK) overnight at 4 °C. The epidermis was gently removed and fixed in 10% neutral buffered formalin (Bio Optica, Milan, Italy) for 2 hours at room temperature; tissue was labeled and mounted as previously described (Braun et al., 2003).

Immunofluorescence labeling

Immunofluorescence on whole mount, frozen, and paraffin-embedded section was performed using standard techniques as previously described (Borgogna et al., 2012). For the list of antibodies used, see Supplementary Table S2 (online).

Single cell suspension for flow cytometry and colony-forming efficiency

Tail and back skin was cut into 0.5 cm^2 pieces and dissociated using 2.5 U/ml Dispase (Roche) overnight at 4 °C. The epidermis was gently removed and further dissociated with TrypLE Express Enzyme (ThermoFisher Scientific, Loughborough, UK), and the supernatant passed through a 70 μm cell strainer (BD Biosciences, Oxford, UK). Enzymes were inactivated with DMEM with 10% fetal bovine serum and keratinocyte cell suspension was resuspended as required.

Flow cytometry, cell sorting, and colony-forming efficiency assay

Samples were analyzed and flow sorted using BD LSRFORTESSA and BD FACSAria Fusion (BD Biosciences). The data were analyzed using FlowJo software (Tree Star, Ashland, OR). Keratinocytes were flow sorted for the CD34-/Lrig1+ population, and 3,000 cells per well were seeded in a 6-well plate and cultured for 15 days. Rheinwald and Green Media was changed every 3 days. The colonies were stained with crystal violet 0.05%, scanned with GelCount (Oxford Optronix, Abingdon, UK), and analyzed using ImageJ software (National Institutes of Health, Bethesda, MD).

Reverse transcription-PCR

Mouse skin was homogenized in Trizol (ThermoFisher Scientific). RNA isolation from sorted cells and homogenized tissues was performed with an RNeasy kit and cDNA was synthetized using a QuantiTect Reverse Transcription Kit (Qiagen, Manchester, UK). Semiquantitative reverse transcription-PCR reactions were carried out using GoTaq G2 Green Master Mix (Promega, Southampton, UK) and sequence-specific primers are listed in Supplementary Table S3 (online). Real-time quantitative reverse transcription analysis was performed on the QuantStudio 7 Flex Real-Time PCR System (ThermoFisher Scientific). For the determination of E6 and E7 gene expression levels, SyGreen (PCR Biosystems, London, UK) was used. Cycling conditions were previously described in

Schaper et al. (2005) and De Andrea et al. (2010). Total mouse-specific β-actin was used as the housekeeping gene.

EVER1, EVER2, TAp63, and ΔNp63 transcription levels were analyzed with Taqman probes under standard conditions. Total mouse-specific GAPDH was used as the housekeeping gene. Primer details are described in Supplementary Tables S3 and S4.

Western blotting

One hundred milligrams of shaved back skin was homogenized in 1 ml of radioimmunoprecipitation assay buffer containing 1% Triton X-100, 1% sodium deoxycholate, 0.1% SDS, 1 mM EDTA, 160 mM NaCl, 20 mM Tris-HCl (pH 7.4), and 25 μl/ml Protease Inhibitor Cocktail (Sigma, Dorset, UK). Protein concentrations were analyzed using Pierce BCA Protein Assay (ThermoFisher Scientific). Thirty micrograms of protein lysate was loaded on 8% SDS-PAGE, and transferred to polyvinylidene difluoride membranes (Millipore, Abingdon, UK). For the list of antibodies used, see Supplementary Table S2.

Human tissue samples

Keratosis formalin-fixed and paraffin-embedded tissue sections of patients with EV were analyzed according to the protocol approved by the "Maggiore Hospital" Research Ethics Committee, Italy. Non-EV AK (14-NW-1272) and squamous cell carcinoma (09-WSE-02-1) tissues were obtained after UK NHS R&D, Local Research Ethics Committee approval and informed written consent.

Statistical analysis

Paired *t* tests were used to compare HPV8 and WT litter mates, using GraphPad software (Prism).

CONFLICT OF INTEREST

The authors state no conflict of interest.

ACKNOWLEDGMENTS

This work was supported by grants from the Italian Ministry for University and Research (MIUR) (PRIN 2012 to CB), Compagnia di San Paolo (CSP2014 to CB), Associazione Italiana per la Ricerca sul Cancro (AIRC) (grant IG 2012 and 2016 to MG), Università del Piemonte Orientale (Fondi di ateneo 2015 to MG), and Cancer Research UK grant (2014). Carlotta Olivero fellowship was funded by Compagnia di San Paolo. We would like to thank Dr John Doorbar, University of Cambridge, for providing the anti-E4 antibodies.

AUTHOR CONTRIBUTIONS

GKP and MG designed research; SL, KP, CO, FC, KD, CB, MDA, SH, and HKCT performed research; HP contributed new reagents; SL, CO, CB, MG, and GKP analyzed data; and SL, CO, MG, and GKP wrote the manuscript.

SUPPLEMENTARY MATERIAL

Supplementary material is linked to the online version of the paper at www.jidonline.org, and at http://dx.doi.org/10.1016/j.jid.2017.04.039.

REFERENCES

Abbas O, Richards JE, Yaar R, Mahalingam M. Stem cell markers (cytokeratin 15, cytokeratin 19 and p63) in in situ and invasive cutaneous epithelial lesions. Mod Pathol 2011;24:90–7.

Azzimonti B, Mondini M, De Andrea M, Gioia D, Dianzani U, Mesturini R, et al. CD8+ T-cell lymphocytopenia and lack of EVER mutations in a patient with clinically and virologically typical epidermodysplasia verruciformis. Arch Dermatol 2005;141:1323–5.

Banerjee M, Sarma N, Biswas R, Roy J, Mukherjee A, Giri AK. DNA repair deficiency leads to susceptibility to develop arsenic-induced premalignant skin lesions. Int J Cancer 2008;123:283–7.

Bernard HU, Burk RD, Chen Z, van Doorslaer K, zur Hausen H, de Villiers EM. Classification of papillomaviruses (PVs) based on 189 PV types and proposal of taxonomic amendments. Virology 2010;401:70–9.

Borgogna C, Landini MM, Lanfredini S, Doorbar J, Bouwes Bavinck JN, Quint KD, et al. Characterization of skin lesions induced by skin-tropic α- and β-papillomaviruses in a patient with epidermodysplasia verruciformis. Br J Dermatol 2014a;171:1550–4.

Borgogna C, Lanfredini S, Peretti A, De Andrea M, Zavattaro E, Colombo E, et al. Improved detection reveals active β-papillomavirus infection in skin lesions from kidney transplant recipients. Mod Pathol 2014b;27:1101–15.

Borgogna C, Zavattaro E, De Andrea M, Griffin HM, Dell'Oste V, Azzimonti B, et al. Characterization of beta papillomavirus E4 expression in tumours from epidermodysplasia verruciformis patients and in experimental models. Virology 2012;423:195–204.

Bosch FX, Broker TR, Forman D, Moscicki AB, Gillison ML, Doorbar J, et al. Comprehensive control of human papillomavirus infections and related diseases. Vaccine 2013;31(suppl 7):H1–31.

Bouwes Bavinck JN, Plasmeijer EI, Feltkamp MC. Beta-papillomavirus infection and skin cancer. J Invest Dermatol 2008;128:1355–8.

Boxman IL, Berkhout RJ, Mulder LH, Wolkers MC, Bouwes Bavinck JN, Vermeer BJ, et al. Detection of human papillomavirus DNA in plucked hairs from renal transplant recipients and healthy volunteers. J Invest Dermatol 1997;108:712–5.

Braun KM, Niemann C, Jensen UB, Sundberg JP, Silva-Vargas V, Watt FM. Manipulation of stem cell proliferation and lineage commitment: visualisation of label-retaining cells in wholemounts of mouse epidermis. Development 2003;130:5241–55.

De Andrea M, Rittà M, Landini MM, Borgogna C, Mondini M, Kern F, et al. Keratinocyte-specific Stat3 heterozygosity impairs development of skin tumors in human papillomavirus 8 transgenic mice. Cancer Res 2010;70:7938–48.

Howley PM, Pfister HJ. Beta genus papillomaviruses and skin cancer. Virology 2015;479–480:290–6.

Hufbauer M, Biddle A, Borgogna C, Gariglio M, Doorbar J, Storey A, et al. Expression of betapapillomavirus oncogenes increases the number of keratinocytes with stem cell-like properties. J Virol 2013;87:12158–65.

Jensen KB, Collins CA, Nascimento E, Tan DW, Frye M, Itami S, et al. Lrig1 expression defines a distinct multipotent stem cell population in mammalian epidermis. Cell Stem Cell 2009;4:427–39.

Jensen KB, Watt FM. Single-cell expression profiling of human epidermal stem and transit-amplifying cells: Lrig1 is a regulator of stem cell quiescence. Proc Natl Acad Sci USA 2006;103:11958–63.

Jonason AS, Kunala S, Price GJ, Restifo RJ, Spinelli HM, Persing JA, et al. Frequent clones of p53-mutated keratinocytes in normal human skin. Proc Natl Acad Sci USA 1996;93:14025–9.

Koster MI. p63 in skin development and ectodermal dysplasias. J Invest Dermatol 2010;130:2352–8.

Kranjec C, Doorbar J. Human papillomavirus infection and induction of neoplasia: a matter of fitness. Curr Opin Virol 2016;20:1–8.

Kretzschmar K, Watt FM. Markers of epidermal stem cell subpopulations in adult mammalian skin. Cold Spring Harb Perspect Med 2014;4:a013631.

Landini MM, Borgogna C, Peretti A, Colombo E, Zavattaro E, Boldorini R, et al. α- and β-papillomavirus infection in a young patient with an unclassified primary T-cell immunodeficiency and multiple mucosal and cutaneous lesions. J Am Acad Dermatol 2014;71:108–15.

Liefer KM, Koster MI, Wang XJ, Yang A, McKeon F, Roop DR. Down-regulation of p63 is required for epidermal UV-B-induced apoptosis. Cancer Res 2000;60:4016–20.

Marcuzzi GP, Hufbauer M, Kasper HU, Weissenborn SJ, Smola S, Pfister H. Spontaneous tumour development in human papillomavirus type 8 E6 transgenic mice and rapid induction by UV-light exposure and wounding. J Gen Virol 2009;90(Pt 12):2855–64.

Melino G. p63 is a suppressor of tumorigenesis and metastasis interacting with mutant p53. Cell Death Differ 2011;18:1487–99.

Melino G, Memmi EM, Pelicci PG, Bernassola F. Maintaining epithelial stemness with p63. Sci Signal 2015;8:re9.

Meyers JM, Spangle JM, Munger K. The human papillomavirus type 8 E6 protein interferes with NOTCH activation during keratinocyte differentiation. J Virol 2013;87:4762–7.

Notarangelo L, Casanova JL, Fischer A, Puck J, Rosen F, Seger R, et al. International Union of Immunological Societies Primary Immunodeficiency Diseases Classification Committee. Primary immunodeficiency diseases: an update. J Allergy Clin Immunol 2004;114:677–87.

Pellegrini G, Dellambra E, Golisano O, Martinelli E, Fantozzi I, Bondanza S, et al. p63 identifies keratinocyte stem cells. Proc Natl Acad Sci USA 2001;98:3156–61.

Pfefferle R, Marcuzzi GP, Akgul B, Kasper HU, Schulze F, Haase I, et al. The human papillomavirus type 8 E2 protein induces skin tumors in transgenic mice. J Invest Dermatol 2008;128:2310–5.

Quint KD, Genders RE, de Koning MNC, Borgogna C, Gariglio M, Bouwes Bavinck JN, et al. Human Beta-papillomavirus infection and keratinocyte carcinomas. J Pathol 2015;235:342–54.

Ramoz N, Rueda LA, Bouadjar B, Montoya LS, Orth G, Favre M. Mutations in two adjacent novel genes are associated with epidermodysplasia verruciformis. Nat Genet 2002;32:579–81.

Schaper ID, Marcuzzi GP, Weissenborn SJ, Kasper HU, Dries V, Smyth N, et al. Development of skin tumors in mice transgenic for early genes of human papillomavirus type 8. Cancer Res 2005;65:1394–400.

Slaughter DP, Southwick HW, Smejkal W. 'Field cancerisation' in oral stratified squamous epithelium. Cancer 1953;6:963–8.

Solanas G, Benitah SA. Regenerating the skin: a task for the heterogeneous stem cell pool and surrounding niche. Nat Rev Mol Cell Biol 2013;14:737–48.

Stockfleth E, Ortonne J-P, Alomar A. Actinic keratosis and field cancerisation. Eur J Dermatol 2011;21:3–12.

Taguchi M, Watanabe S, Yashima K, Murakami Y, Sekiya T, Ikeda S. Aberrations of the tumor suppressor p53 gene and p53 protein in solar keratosis in human skin. J Invest Dermatol 1994;103:500–3.

Truong AB, Kretz M, Ridky TW, Kimmel R, Khavari PA. p63 regulates proliferation and differentiation of developmentally mature keratinocytes. Genes Dev 2006;20:3185–97.

Vasilaki E, Morikawa M, Koinuma D, Mizutani A, Hirano Y, Ehata S, et al. Ras and TGF-β signaling enhance cancer progression by promoting the ΔNp63 transcriptional program. Sci Signal 2016;9:ra84.

Viarisio D, Mueller-Decker K, Kloz U, Aengeneyndt B, Kopp-Schneider A, Gröne HJ, et al. E6 and E7 from beta HPV38 cooperate with ultraviolet light in the development of actinic keratosis-like lesions and squamous cell carcinoma in mice. PLoS Pathog 2011;7:e1002125.

Weissenborn SJ, Nindl I, Purdie K, Harwood C, Proby C, Breuer J, et al. Human papillomavirus-DNA loads in actinic keratoses exceed those in non-melanoma skin cancers. J Invest Dermatol 2005;125:93–7.

Yang A, Kaghad M, Wang Y, Gillett E, Fleming MD, Dötsch V, et al. p63, a p53 homolog at 3q27-29, encodes multiple products with transactivating, death-inducing, and dominant-negative activities. Mol Cell 1998;2:305–16.

Yang A, Schweitzer R, Sun D, Kaghad M, Walker N, Bronson RT, et al. p63 is essential for regenerative proliferation in limb, craniofacial and epithelial development. Nature 1999;398:714–8.